R-matrix study of elastic and inelastic electron collisions with cytosine and thymine

2012 J. Phys. B: At. Mol. Opt. Phys. 45 175203

(http://iopscience.iop.org/0953-4075/45/17/175203)

J. Phys. B: At. Mol. Opt. Phys. **45** (2012) 175203 (9pp) doi:10.1088/0953-4075/45/17/175203

R-matrix study of elastic and inelastic electron collisions with cytosine and thymine

Amar Dora[1,2], **Lilianna Bryjko**[3], **Tanja van Mourik**[3] **and Jonathan Tennyson**[1]

[1] Department of Physics and Astronomy, University College London, Gower Street, London WC1E 6BT, UK
[2] Laboratoire Aimé Cotton du CNRS, Universite de Paris-Sud, 91405 Orsay, France
[3] School of Chemistry, University of St. Andrews, North Haugh, St. Andrews, Fife KY16 9ST, UK

E-mail: j.tennyson@ucl.ac.uk

Received 13 April 2012, in final form 6 July 2012
Published 9 August 2012
Online at stacks.iop.org/JPhysB/45/175203

Abstract

Ab initio scattering calculations for low-energy electron collisions with gas-phase DNA pyrimidine bases (cytosine and thymine) are performed using the **R**-matrix method. The low-lying resonant states of the anions, formed due to electron capture by the bases, are identified using different levels of theory, including static exchange, static exchange plus polarization, and close-coupling approximations. For both the bases, all of our scattering models find three shape resonances of $^2A''$ (π) symmetry lying below 10 eV, in accordance with other calculations and experimental observations. In addition to these, a fourth $^2A''$ resonance is found in all models for thymine and in our best model, i.e. the uncontracted close-coupling approximation, for cytosine. This model places the fourth $^2A''$ resonance in both systems in the 6–7 eV range. No evidence is found for the presence of low-lying Feshbach resonances in either system. Integral cross sections for electronically elastic and inelastic collisions are also presented.

(Some figures may appear in colour only in the online journal)

1. Introduction

The discovery that electron collisions at energies below the excitation and ionization thresholds are associated with strand breaks in DNA (Boudaïffa *et al* 2000) has continued to attract considerable interest. The rupture of DNA strands is thought to proceed from the attachment of an electron to a particular site within the DNA molecule, forming a metastable anionic complex. This anion can subsequently dissociate in various possible ways. The first step in understanding these processes requires the identification of the under-lying metastable or resonant anionic states that could be the drivers of this mechanism.

To this end, several experimental groups (Denifl *et al* 2004, Ptasińska *et al* 2005, Hanel *et al* 2003, Denifl *et al* 2003, Scheer *et al* 2004, 2005, Aflatooni *et al* 2005, Abouaf and Dunet 2005, Burrow *et al* 2006) have measured cross sections for the creation of anionic fragments of DNA/RNA components produced through dissociative attachment (DA) processes. Other experimental studies focussed on measuring the attachment energies of electrons to the nucleic acid bases in their gas phases by electron transmission spectroscopy (ETS) (Aflatooni *et al* 1998).

Theoretical studies that aim to identify the possible resonant states of isolated DNA/RNA fragments have also appeared in the literature. These include calculations on phosphoric acid (Tonzani and Greene 2006b, Winstead and McKoy 2008a, Bryjko *et al* 2010) and tetrahydrofuran (Bouchiha *et al* 2006, Trevisan *et al* 2006, Tonzani and Greene 2006b), as models for the phosphate and pentose sugar moieties, respectively, that together make the DNA/RNA backbone. In addition, a recent time-dependent dynamics study (Renjith *et al* 2011) employed a modelled local complex potential for single-strand breakage of a DNA fragment

containing the base-sugar-phosphate group. The nucleic acid bases, which are likely to be the favourable candidates for electron attachment due to the presence of low-lying empty molecular orbitals (MOs), have also been studied by several groups (Winstead and McKoy 2006a, 2006b, 2008b, Dora *et al* 2009, 2012, Winstead and McKoy 2007a, Tonzani and Greene 2006a, Gianturco *et al* 2008, Wang and Tian 2011). The associated fundamental research, both experimental and theoretical, on radiation damage following electron attachment to DNA has recently been extensively reviewed (Baccarelli *et al* 2011, García Gómez-Tejedor and Fuss 2012).

Resonant states of different types and characters are possible depending upon the mechanism of electron capture by the molecular target. Resonant anions formed by temporary trapping of a scattering electron through a barrier in the electron–molecule interaction potential are called shape resonances. Shape resonances associated with trapping of the electron by the molecular ground state are described by the occupation of the extra electron in one of the low-lying empty MOs. The parameters characterizing shape resonances are known to be very sensitive to the treatment of polarization effects.

When the scattering process causes electronic excitation of the target, the electron can be trapped by the potential barrier, giving rise to a core-excited shape resonance. These shape resonances lie energetically above their respective parent electronic states and decay predominantly to their parent states by tunnelling of the electron through the potential barrier. Another class of core-excited resonance, known as Feshbach resonance, occurs when the electron is trapped at energies below the associated parent excited state. This indicates that the parent state associated with a Feshbach resonance has a positive electron affinity. The electronic configuration of both core-excited shape resonances and Feshbach resonances involves a hole in the normally occupied valence orbitals and two electrons in unoccupied (or virtual) orbitals of the target. Therefore, it can be hard to distinguish a Feshbach resonance from a core-excited shape resonance solely based on the electronic configuration. However, in contrast to shape resonances, Feshbach resonances generally have long lifetimes, as decay to their parent states is not energetically possible and decay to the lower target states involves a change in electronic configuration. Feshbach and core-excited shape resonances are best treated in close-coupling calculations, which explicitly include the parent target state(s) in the wavefunction.

The classification of resonance state types as described above is not always a strict one. In many-electron systems, identifying and associating a resonance to a particular parent state is a difficult and imprecise task, due to the presence of a large number of excited states within a small energy range (Stibbe and Tennyson 1997). In such cases the electronic structure of a resonance is described by a combination of several configurations built upon many target states. Indeed, it has been established that the highest-lying $\pi^\star$ shape resonance of pyrazine is significantly mixed with core-excited resonances (Winstead and McKoy 2007b, 2007c, Mašín and Gorfinkiel 2011). While shape resonances associated with the ground target state can be described by simpler theoretical treatments by including only the elastic channel, the theoretical description of such mixed resonances should also include coupling to the inelastic decay channels.

To complete our previous studies on isolated DNA/RNA fragments, we report here fixed-nuclei **R**-matrix calculations of low-energy electron scattering by the pyrimidine bases cytosine and thymine. As in our earlier works, several scattering models, representing different degrees of polarization, have been used to characterize the resonances in the collisions. For our best model, which includes both the elastic and the electronic excitation channels, we report total elastic and electron impact excitation cross sections. There have been only a few other theoretical studies on these molecules. These studies, which include the single-centre model potential scattering calculations of Tonzani and Greene (2006a), and the Schwinger multi-channel (SMC) static exchange and static exchange plus polarization calculations by Winstead and McKoy (2007a), only considered the elastic scattering channel.

2. Computational details

We use the **R**-matrix method as implemented in the UK polyatomic **R**-matrix codes (Morgan *et al* 1998). We note that the codes themselves have recently been extensively re-written and modernized (Carr *et al* 2012). The **R**-matrix method is a widely applied *ab initio* procedure for studying electron scattering with atomic and molecular targets (Burke 2011). The theory and its numerical implementation in the UK molecular **R**-matrix codes has been described before in the literature, and was recently reviewed extensively by one of us (Tennyson 2010). We therefore omit the theory part and only mention the computational aspects related to the present work.

In the following sections, we present results from calculations employing four different scattering models. These are the static exchange (SE), SE plus polarization (SEP), close-coupling (CC) and the uncontracted close-coupling (u-CC) models. These models have been described in detail in our previous works (Dora *et al* 2009, 2012) and they correspond to different levels of theoretical treatment of electron correlation and polarization in the target and the scattering systems. Extensive tests on the effects of the basis set size, **R**-matrix radius, inclusion of virtual orbitals and method used to generate them, as well as other parameters in the calculations, were reported as part of our study on electron collisions with uracil (Dora *et al* 2009). Below, we describe the specific set of computational parameters used in the current study.

2.1. Target calculations

Cytosine and thymine can exist in many different tautomeric forms. Here, we use the tautomers that are most stable in the gas phase (Caminati 2009). The ground state nuclear geometries of these tautomers are obtained by geometry optimization using density functional theory (DFT) with the B3LYP functional and the 6−31+G* basis set, employing the GAUSSIAN-03 package (Frisch *et al* 2004). To take advantage of the

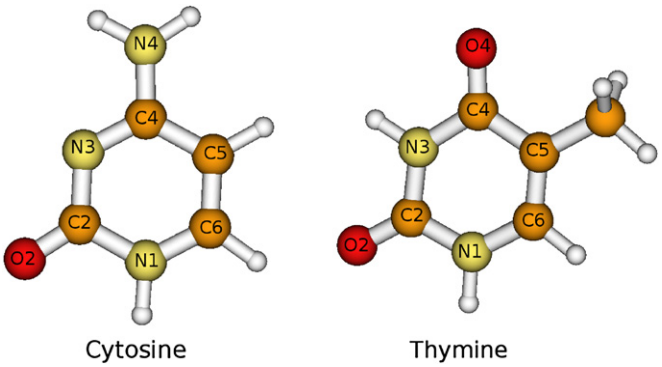

Figure 1. The structures of cytosine and thymine considered in this work.

computational and analytical simplifications in the presence of molecular symmetry, the geometry optimization was done by imposition of C_s point group symmetry. With this restriction, both molecules have planar structures with the exception of two H-atoms of the methyl group in thymine, which lie outside the molecular plane in opposite directions (see figure 1). We note that the planar cytosine structure is a first-order transition state (one imaginary frequency); the optimized nonplanar cytosine molecule is a minimum and possesses a slightly lower energy (-394.949754 E_h) than its planar counterpart (-394.949726 E_h). In the case of thymine, the C_s symmetric structure is a true minimum (no imaginary frequencies) with an energy of -454.158106 E_h. The ground-state electronic configuration, in C_s symmetry, of cytosine is $(1a' - 24a')^{48}(1a'' - 5a'')^{10}$ and that of thymine is $(1a' - 27a')^{54}(1a'' - 6a'')^{12}$.

Initially several basis sets, including 6-31G, cc-pVDZ, and cc-pVTZ, were tested to investigate the stability of target properties such as the dipole moment and vertical electronic excitation. We finally chose the cc-pVDZ basis set, to keep the computationally demanding scattering calculations tractable. It should be noted that in a recent **R**-matrix calculation on electron scattering from pyrazine, Mašín and Gorfinkiel (2011) observed that the use of basis sets containing diffuse functions gave better scattering results compared to the compact basis sets used here. In particular, they found that the diffuse basis set gave a better representation of the target virtual orbitals in the complete active space self-consistent field (CASSCF) calculations. However, the use of diffuse one-electron functions for a large molecule like pyrazine required the use of a larger **R**-matrix radius of 18 a_0; such calculations encounter problems with linear dependence and reduced energy range (see Tarana and Tennyson (2008) for a discussion of this). For this reason we have not attempted to use a diffuse basis set for cytosine and thymine, which are bigger in size than pyrazine; all the results reported in this paper were obtained with the cc-pVDZ basis set.

In the SE and SEP models the target is represented only by the ground-state Hartree–Fock (HF) wavefunction, while in the CC models several target states, represented at a partially correlated level of a complete active space configuration interaction (CAS-CI) model (Tennyson 1996), are included. Several target calculations with different active spaces and a different number of states represented using orbitals generated from a state-averaged CASSCF (SA-CASSCF) procedure were tried for both molecules as part of their convergence tests. We found that an active space of 14 valence electrons distributed over 10 orbitals (in short notation, CASSCF(14,10)) and 20 states (five states from each space-spin symmetry) in the SA-CASSCF procedure gave convergence for both molecules. Specifically, the chosen active spaces correspond, for cytosine, to the $(1a' - 22a')^{44}$, $(23a' - 24a', 1a'' - 8a'')^{14}$ configuration and for thymine to the $(1a' - 25a', 1a'')^{52}$, $(26a' - 27a', 2a'' - 9a'')^{14}$ configuration. The use of bigger active spaces than this is currently unmanageable in the scattering calculations. These HF and SA-CASSCF calculations were performed using the MOLPRO 2006.1 (Werner *et al* 2006) package. The MOs obtained from the MOLPRO calculations were used to construct the target wavefunctions and the L^2 configurations in the scattering calculations by the UK **R**-matrix codes.

The HF ground-state energy and dipole moment are, for cytosine, -392.637258 E_h and 8.29 D, respectively, whereas the corresponding values for thymine are -451.545218 E_h and 4.74 D. In the CC calculations of both molecules we used all the 20 SA-CASSCF target states in the expansion. Table 1 contains the SA-CASSCF ground-state energies, vertical excitation energies for excitation to the remaining 19 excited states and the ground-state dipole moments of cytosine and thymine. For comparison, the CASSCF/CASPT2 vertical excitation energies and ground-state dipole moments from Fülscher and Roos (1995) and Lorentzon *et al* (1995) are also included in the table. In most cases, our results agree well with the other CASSCF data. For thymine, the differences between the different CASSCF calculations are within ~0.6 eV. As a general trend, our vertical excitation energies are somewhat smaller for low-lying excited states and larger for higher-lying excited states of a particular symmetry. The largest difference between the calculations occurs for excitation to the $2\,^1A''$ state of cytosine where our value is 1.6 eV smaller than the CASSCF result of Fülscher and Roos (1995). The differences between these calculations can be attributed to differences in the active spaces, basis sets and molecular geometries. The vacuum ultraviolet (VUV) absorption bands, corresponding to excitations to the low-lying singlet states, observed by various optical spectra (Fülscher and Roos 1995, Lorentzon *et al* 1995, Varsano *et al* 2006) along with the excitation energies derived from electron energy loss spectroscopy (EELS) in the gas phase (Abouaf *et al* 2003, 2004) and in deposited films (Levesque *et al* 2005, Bazin *et al* 2010) are also included in table 1. In the context of table 1, we note that it is not always possible to assign a theoretical spatial symmetry to the experimentally observed vertically excited states.

2.2. Scattering calculations

In all scattering models we used an **R**-matrix sphere of radius $a = 13$ a_0. We used continuum Gaussian-type orbitals with partial waves up to $\ell \leqslant 4$, as optimized for this sphere size by Faure *et al* (2002). The contribution from higher partial waves to the elastic and electron impact excitation cross sections

Table 1. Ground state ($X\ ^1A'$) energies (in E_h), dipole moments (in D) and vertical excitation energies (in eV) of cytosine and thymine obtained with the CASSCF(14,10) model with the cc-pVDZ basis set. The results of other *ab initio* calculations, as well as experimental values, are also shown.

	Cytosine					Thymine				
State	This work	CASSCF[a]	CASPT2[a]	VUV[b]	EELS (gas[c]/film[d])	This work	CASSCF[e]	CASPT2[e]	VUV[f]	EELS (gas[g]/film[h])
$X\ ^1A'$	−392.69113					−451.60520				
$2\ ^1A'$	4.75	5.18	4.39	4.5−4.6	4.65/4.65	6.63	6.75	4.88	4.5−4.7	4.95/...
$3\ ^1A'$	6.48	6.31	5.36	5.0−5.3	5.50/5.39	7.17	7.15	5.88	5.0−5.1	6.2/...
$4\ ^1A'$	8.06	7.30	6.16	5.4−5.8	6.20/6.18	8.63	8.33	6.10	5.8−6.0	
$5\ ^1A'$	8.17	7.82	6.74	6.1−6.3	6.70/6.83	9.25	8.62	7.13	6.3−6.6	7.4/...
$1\ ^1A''$	4.76	5.13	5.00	6.7−7.1	.../5.01	4.97	5.22	4.39	7.0	
$2\ ^1A''$	5.57	7.14	6.35			6.59	6.77	5.91		
$3\ ^1A''$	5.64					7.96	8.14	6.15		
$4\ ^1A''$	7.98					8.10	8.41	6.70		
$5\ ^1A''$	9.23					10.11				
$1\ ^3A'$	3.53				3.50/3.55	3.84				3.6/3.7
$2\ ^3A'$	4.63				4.25/4.02	5.51				.../4.9
$3\ ^3A'$	5.39					6.39				.../6.0
$4\ ^3A'$	6.92					7.73				.../6.3
$5\ ^3A'$	7.93					8.64				.../7.3
$1\ ^3A''$	4.65					4.80				.../4.0
$2\ ^3A''$	5.35					6.40				
$3\ ^3A''$	5.55					7.85				
$4\ ^3A''$	7.98					8.07				
$5\ ^3A''$	9.10					10.04				
$\mu(X\ ^1A')$	6.33	7.35				3.98	5.0			

[a] From Fülscher and Roos (1995).
[b] Experimental absorption bands and their references as collected by Fülscher and Roos (1995) and Varsano *et al* (2006).
[c] Excitation energies from gas-phase EELS of Abouaf *et al* (2004).
[d] Excitation energies from condensed-phase EELS of Bazin *et al* (2010).
[e] From Lorentzon *et al* (1995).
[f] Experimental absorption bands and their references as collected by Fülscher and Roos (1995) and Varsano *et al* (2006).
[g] Excitation energies from gas-phase EELS of Abouaf *et al* (2003).
[h] Excitation energies from condensed-phase EELS of Levesque *et al* (2005).

($\ell > 4$) has been calculated for our best model, i.e. the u-CC model, by using the Born approximation (Chu and Dalgarno 1974) as implemented in the routine BORNCROSS (Baluja *et al* 2000). This treatment takes care of the target rotational motion, within the rigid rotor approximation, which acts to average out the effects of the asymptotic dipole potential.

In previous **R**-matrix calculations with small biomolecules (Bouchiha *et al* 2006, Dora *et al* 2009, Bryjko *et al* 2010, Mašín and Gorfinkiel 2011, Dora *et al* 2012) it was found that the number of target virtual MOs retained in the calculations was crucial for getting the resonance positions closer to the observed values. In the current study we used 15 virtual orbitals from each symmetry (i.e. 30 virtual MOs in total) for all models. With this choice we found good agreement between the u-CC results and the observed data (Aflatooni *et al* 1998). The use of 30 virtual MOs in the u-CC model produced a large number of configuration state functions (CSFs), i.e. 181464 A'' and 181276 A' CSFs for both cytosine and thymine. To deal with the diagonalization of the large Hamiltonian matrices resulting from this, we use the partitioned **R**-matrix method (Tennyson 2004), which requires only a small proportion of the eigen-solutions of the full scattering Hamiltonian (significantly less than 10%). In this study we used the lowest 5000 eigen-solutions for the u-CC calculations; this choice typically takes around 10 days to complete the calculation for each symmetry on a 64-bit, 4-core workstation using a parallel version of the code optimized for this task as discussed by Zhang *et al* (2011).

The scattering eigenphase sums and cross sections were evaluated on a fine grid of incident electron energy. Identification of any possible resonances and estimation of their positions and widths utilized the automated Breit–Wigner profile fitting program RESON (Tennyson and Noble 1984). However, in some cases the fitting of eigenphase sums to the Breit–Wigner profile failed (particularly for resonances at higher energies in the close-coupling models). In such cases we estimated the resonance positions from the eigenphase sum and the total cross section plots.

3. Results and discussion

Electron collision calculations on cytosine and thymine identified several shape resonances of A'' (π) symmetry, in agreement with calculations on other heteronuclear aromatic systems (including uracil, adenine, guanine and pyrazine). All scattering models revealed at least three A'' resonances below 10 eV for both thymine and cytosine. In addition to these, a

Table 2. Positions (and widths) of low-lying A'' (or π) shape resonances for cytosine and thymine. All quantities are in eV.

Bases	Reference	Model	$A''(\pi)$-resonances			
Cytosine	This work	SE	2.65 (0.34)	4.69 (0.67)	9.85 (2.08)	
	Tonzani and Greene (2006a)	SE	1.70 (0.50)	4.30 (0.70)	8.10 (0.80)	
	This work	SEP	0.71 (0.05)	2.66 (0.33)	6.29 (0.72)	
	Winstead and McKoy (2007a)[a]	SEP	0.50	2.40	6.30	
	This work	CC	1.20 (0.06)	3.02 (0.42)	6.08 (1.39)	
	This work	u-CC	0.36 (0.016)	2.05 (0.30)	5.35[c]	6.78[c]
	Aflatooni *et al* (1998)[b]	Obs.	0.32	1.53	4.50	
Thymine	This work	SE	2.45 (0.36)	4.60 (0.27)	7.98 (1.55)	11.41 (1.06)
	Tonzani and Greene (2006a)	SE	2.40 (0.20)	5.50 (0.60)	7.90 (1.00)	
	This work	SEP	0.60 (0.11)	2.73 (0.11)	5.52 (0.57)	7.41(0.12)
	Winstead and McKoy (2007a)[a]	SEP	0.30	1.90	5.70	
	This work	CC	1.38 (0.15)	3.34 (0.16)	6.34 (0.45)	7.54[c]
	This work	u-CC	0.53 (0.08)	2.41 (0.10)	5.26[c]	6.23[c]
	Aflatooni *et al* (1998)[b]	Obs.	0.29	1.71	4.05	

[a] No widths reported.
[b] Observed (ETS) vertical attachment energies.
[c] Resonance position estimated from our total cross section peaks.

fourth $^2A''$ resonance is found in all models for thymine and in the u-CC model for cytosine. Their positions and widths are presented in table 2. Also included are the results of other available calculations as well as experimental attachment energies obtained through ETS (Aflatooni *et al* 1998).

Ignoring small differences, table 2 shows a fair amount of similarity in the positions and widths of the resonances within a particular scattering model. This similarity also extends to the resonances in the RNA pyrimidine base uracil, which has the same structure of thymine but with the methyl group replaced by hydrogen. It appears that the cyclic delocalization of the attached electron helps to stabilize the π resonances in these aromatic systems. Therefore, the base's π-ring orbitals are probably mainly responsible for the attachment of electrons at certain energies with only little perturbatory contributions from the groups attached to the ring.

The SE approximation, in which the target is frozen in its ground electronic state and not allowed to polarize in the presence of the scattering electron, places the resonances in both systems at higher energies and provides an upper limit to these. With successively better calculations with polarization included these positions get lowered, as is expected in a variational calculation. However, our SE positions are in quantitative agreement with the SMC calculations of Winstead and McKoy (2007a), who did not provide the exact values for their SE results. The **R**-matrix calculation of Tonzani and Greene (2006a), which uses a one-electron scattering model and simple local approximations to the exchange and polarization effects, gives resonance positions somewhat lower than our SE results for cytosine, but a little higher for thymine.

Inclusion of polarization effects via the SEP model lowers the resonance positions and moves them towards the observed values (Aflatooni *et al* 1998). However, our SEP resonance positions are still higher than the SEP results of Winstead and McKoy (2007a) and the observed values (Aflatooni *et al* 1998). As we mentioned above and demonstrated in our uracil calculations (Dora *et al* 2009), including a larger number of virtual MOs in the polarization calculation results in lower resonance positions. In the present SEP calculations we used 15 virtual MOs from each symmetry. The difference between our and the corresponding SEP results of Winstead and McKoy (2007a) may be due to a more complete treatment of polarization in the latter calculations.

The CC calculation uses a large expansion for the scattering wavefunction and takes 20 target states (the lowest five states from each spin-symmetry) represented at the CAS-CI level. In the simpler CC model, L^2 CSFs with the 'extra' electron in a virtual orbital are contracted with the target CAS-CI in the same manner as continuum orbitals (see Tennyson (1996) for details). This model was found not to lower the resonance positions much; it is known that convergence with respect to the target state expansion is very slow in this model. However, this convergence is accelerated in the u-CC model, which does not contract the L^2 CSFs. We get good agreement with the lowest observed resonance position in both cytosine and thymine with the inclusion of 15 virtual MOs from each symmetry in the u-CC model and an expansion of 20 target states. However, the second and third resonance positions are still too high by 0.5–1.2 eV in both systems. Inclusion of further virtual MOs in the calculations, to recover correlation in the higher-lying resonances, would bring down their positions towards the observed data. However, this would deteriorate the balance of correlation in the first resonance with the target and would probably result in the first resonance appearing at negative energy. In our CC calculation on adenine (Dora *et al* 2012) we found that a larger active space in the CASSCF representation of the target states leads to a decrease in the resonance positions. However, the use of active spaces larger than the one we have employed here in the scattering calculations is currently unmanageable. For pyrazine it has been shown (Winstead and McKoy 2007b, 2007c, Mašín and Gorfinkiel 2011), that the highest-lying π resonance is partially mixed with electronic excitation channels. As we show below, this is also the case for the higher-lying π resonances in cytosine and thymine. Therefore, a better treatment of correlation and polarization effects is expected to improve the description of these mixed resonances.

There are no reports in the literature of $^2A'$ symmetry resonances in cytosine or thymine. The presence of resonances

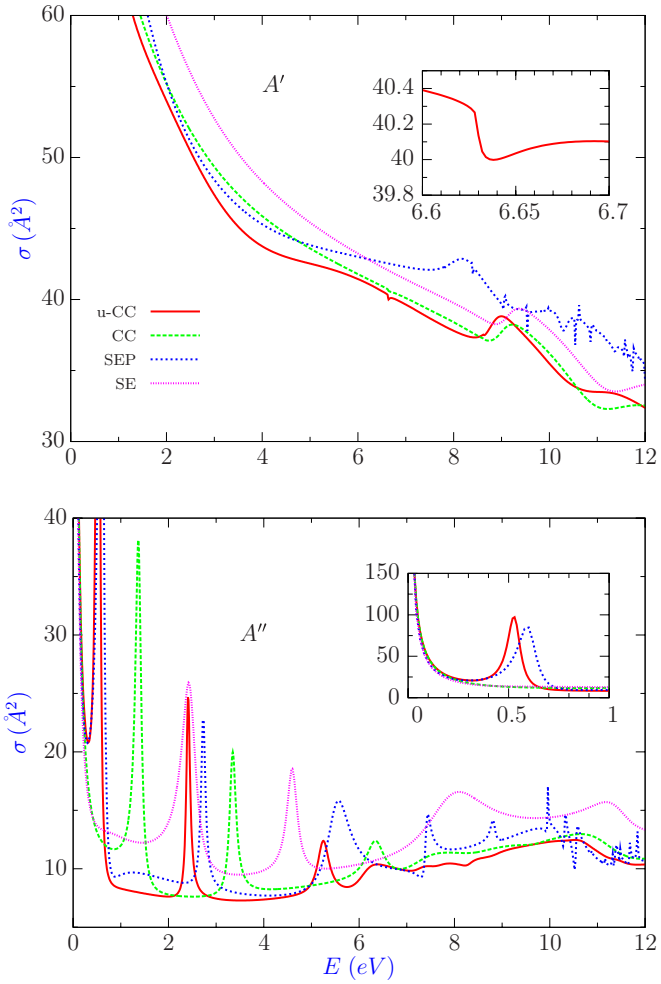

Figure 2. Elastic cross sections of electron collision with thymine. The contributions from the A' and A'' symmetry are shown separately to identify the resonances. The inset figure for A'' symmetry shows the low-energy behaviour for all models used and the sharp peak at 0.53 eV in the u-CC model. The inset for A' symmetry shows the effect of the resonance at 6.65 eV found in the u-CC model.

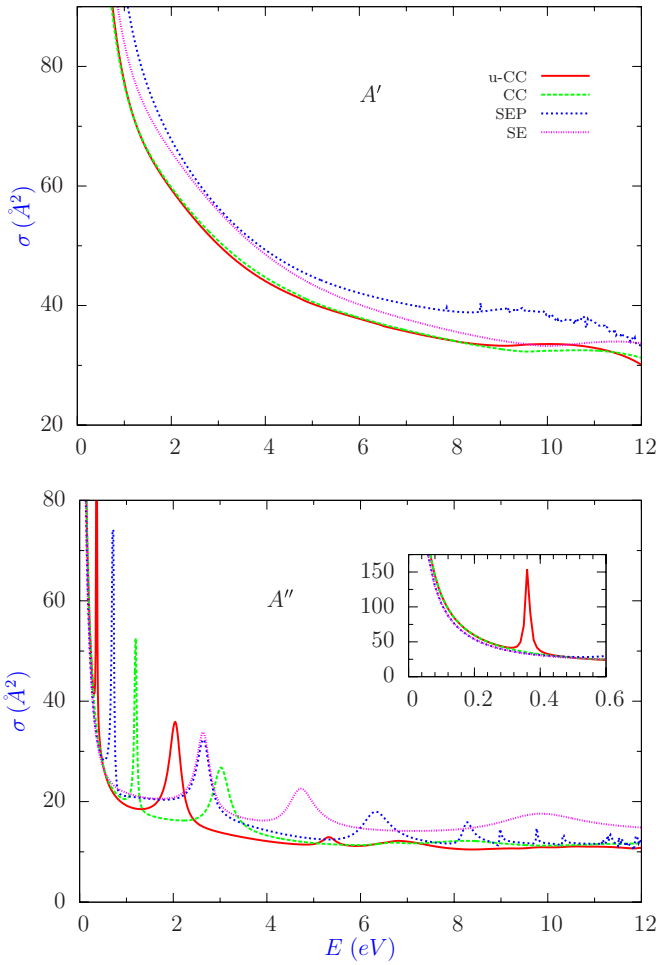

Figure 3. Elastic cross sections of electron collision with cytosine. Contributions from the A' and A'' symmetry are shown separately to identify the resonances in different models. The inset figure for A'' symmetry shows the low-energy behaviour for all models used and the sharp peak at 0.36 eV for the u-CC model.

in either system is not clear-cut from our $^2A'$ calculations, since they appear inconsistently among the models and at higher energies, where it is harder to get good results. In the u-CC calculation for thymine the lowest-lying resonance-like structure we find is at around 6.65 eV, see the drop in A' contribution to the elastic cross section around 6.64 eV in the inset of figure 2. At this position the A' eigenphase sum also shows a definite jump, which however is not identified as a resonance in the automatic eigenphase fitting program RESON. No narrow $^2A'$ resonances are found in these calculations. In our previous calculations on uracil (Dora *et al* 2009), adenine (Dora *et al* 2012) and H_3PO_4 (Bryjko *et al* 2010) we found some very narrow $^2A'$ resonances, which appeared only in the models with enhanced treatment of polarization. We suggested these resonance have Feshbach character.

The effect of resonances on the elastic cross sections can be seen in figure 3 for cytosine and in figure 2 for thymine, plotted separately for $^2A'$ and $^2A''$ symmetries for all the models employed. The $^2A'$ cross section in cytosine is mostly structureless, except for the SEP model which has many structures due to unphysical pseudoresonances above the threshold for electronic excitation. At higher energies, however, some very broad structures appear in both molecules. Particularly, in the thymine $^2A'$ cross sections there is a persisting broad peak in all models in the 8–10 eV range. Additional overlapping peaks are also seen at higher energies in the $^2A''$ cross sections of both molecules in the CC models.

We note that the eigenphase sum fitting program RESON failed to detect the third and fourth $^2A''$ resonance in both molecules. These resonances lie at energies close to several target excitation thresholds and there are problems associated with eigenphase fitting across excitation thresholds since the derivative of the eigenphase is in general not continuous at threshold. An alternative method using the time-delay to characterize resonances has been described by Stibbe and Tennyson (1996). However, in the present case we estimate the positions of the higher two resonances from their total (elastic + electronic excitation) cross section peaks.

The total $(A' + A'')$ elastic cross sections for electron collisions with cytosine and thymine are presented in figures 4 and 5, respectively, for our final u-CC calculation. The cross

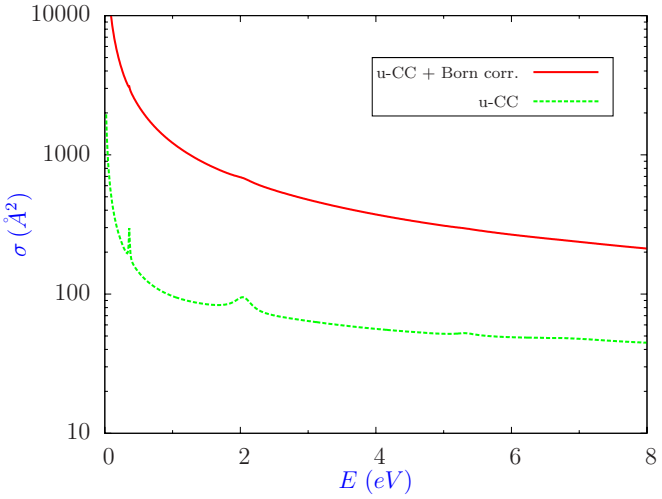

Figure 4. Total elastic cross section for low-energy electron collisions with cytosine in the final uncontracted CC model with and without the Born correction.

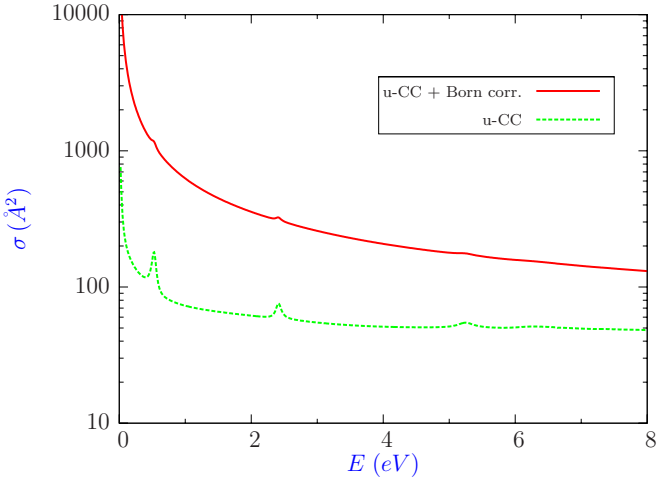

Figure 5. Total elastic cross section for low-energy electron collisions with thymine in the final uncontracted CC model with and without the Born correction.

sections increase rapidly at lower energies as both molecules have large dipole moments. The contribution to the calculated elastic cross section from higher partial waves was computed using the Born approximation and is shown separately in the figures. This huge correction almost completely washes out the peaks due to the resonances. To the best of our knowledge, there have been no measurements on integral or differential elastic cross sections for these systems. For uracil, however, elastic cross section measurements at a 90° scattering angle were reported by Abouaf and Dunet (2005) and reproduced well in our electron collision study (Dora *et al* 2009).

Electron impact electronic excitation of either cytosine or thymine does not appear to have been considered in any previous studies. In figure 6 we present electron impact electronic excitation cross sections for cytosine and in figure 7 for thymine, obtained with the u-CC model. Only excitations to the first two triplet and to the lowest singlet states of A' symmetry are shown. The cross sections for other excitations were found to be very small. For excitations to the singlet state

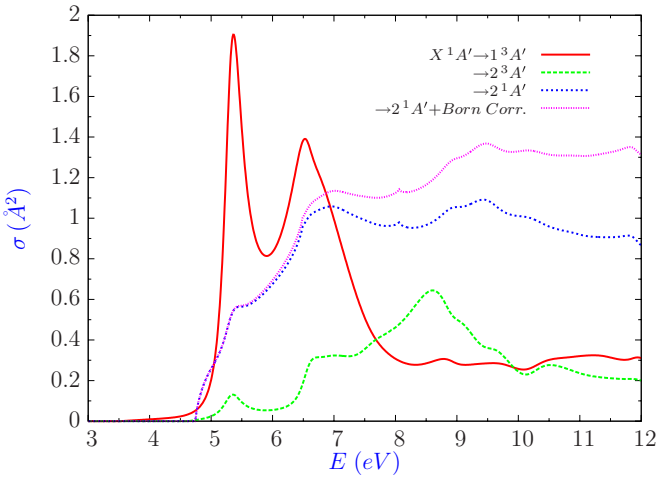

Figure 6. Electron impact excitation cross sections of cytosine to the lowest two triplet A' states and to the $2\,^1A'$ state. For excitation to the singlet state the Born contribution is shown. The excitation cross sections to other higher states and to the A'' states are comparatively very small.

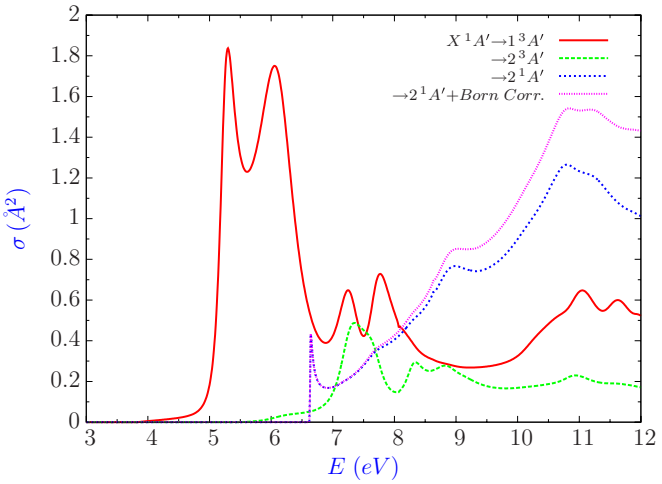

Figure 7. Electron impact excitation cross section of thymine to the lowest two triplet A' states and to the $2\,^1A'$ state. For excitation to the singlet state the Born contribution is shown. The other excitation cross sections are very small.

we have added the Born correction. The sharp peaks at 5.3 and 6.5 eV in the excitation to the first $^3A'$ state in cytosine come exclusively from the $^2A''$ symmetry, indicating that the third and fourth $^2A''$ resonances, respectively at 5.35 and 6.78 eV, are responsible for these. Similarly, the peak structures in the excitation to the $^3A'$ states in thymine is mostly contributed by the $^2A''$ symmetry and are due to the higher-lying $^2A''$ resonances at 5.26 eV, 6.23 eV and above. This indicates that the higher-lying $^2A''$ resonances have partial core-excited shape resonance character. The lower two $^2A''$ resonances in both systems are shape resonances formed due to electron capture by the target in its ground state and they entirely contribute to the elastic channel. The sharp spike structure at 6.64 eV in the excitation to the $^1A'$ state of thymine is entirely due to $^2A'$ symmetry, which indicates the involvement of the $^2A'$ resonance at around 6.65 eV.

4. Conclusion

Calculations are presented for low-energy electron scattering with the pyrimidine bases cytosine and thymine using several *ab initio* models. Theoretical characterization of the low-lying resonances in nucleic acid bases is important for studying their observed DA processes and hence in modelling the radiation damage to DNA.

Below 10 eV, three shape resonances of $^2A''$ symmetry are identified in all our scattering models. We get good agreement with the observed position for the lowest resonance in our best model. The discrepancy for the higher resonances compared to the measurements are due to insufficient treatment of correlation-polarization effects in our calculations. The treatment of polarization effects offered in the molecular **R**-matrix with pseudo-states (RMPS) method (Gorfinkiel and Tennyson 2004, 2005) should be able to resolve this problem. However, RMPS calculations for large molecules like these are computationally very expensive at present, see Zhang *et al* (2011).

In addition to the three $^2A''$ resonances, in our best uncontracted close-coupling model—which treats correlation-polarization effects at a higher level—we find a fourth $^2A''$ resonance around 6.5 eV for both molecules. The two higher-lying resonances in each system are partially coupled with core-excited channels and they contribute towards electron impact excitations. The two lowest shape resonances are due to the target ground state and decay predominantly via the elastic channel. Indications of higher-lying shape resonances of $^2A'$ symmetry are also found in thymine. We found no evidence for low-lying Feshbach resonances in either molecule.

Acknowledgments

This project was funded by the UK Engineering and Physical Sciences Research Council. LB and TvM thank EaStCHEM for computational support via the EaStCHEM Research Computing Facility. AD was supported in part by the ANR (France) under contract no 09-BLAN-020 901 and thanks Ch Jungen for the use of computing facility at Laboratoire Aimé Cotton.

References

Abouaf R and Dunet H 2005 *Eur. Phys. J.* D **35** 405
Abouaf R, Pommier J and Dunet H 2003 *Chem. Phys. Lett.* **381** 486–94
Abouaf R, Pommier J, Dunet H, Quan P, Nam P C and Nguyen M T 2004 *J. Chem. Phys.* **121** 11668
Aflatooni K, Gallup G A and Burrow P D 1998 *J. Phys. Chem.* A **102** 6205
Aflatooni K, Scheer A M and Burrow P D 2005 *Chem. Phys. Lett.* **408** 426
Baccarelli I, Bald I, Gianturco F A, Illenberger E and Kopyra J 2011 *Phys. Rep.* **508** 1–44
Baluja K L, Mason N J, Morgan L A and Tennyson J 2000 *J. Phys. B: At. Mol. Opt. Phys.* **33** L677–84
Bazin M, Michaud M and Sanche L 2010 *J. Chem. Phys.* **133** 155104
Bouchiha D, Gorfinkiel J D, Caron L G and Sanche L 2006 *J. Phys. B: At. Mol. Opt. Phys.* **39** 975–86
Boudaïffa B, Cloutier P, Hunting D, Huels M A and Sanche L 2000 *Science* **287** 1658
Bryjko L, van Mourik T, Dora A and Tennyson J 2010 *J. Phys. B: At. Mol. Opt. Phys.* **43** 235203
Burke P G 2011 *R-Matrix Theory of Atomic Collisions: Application to Atomic, Molecular and Optical Processes* (Berlin: Springer)
Burrow P D, Gallup G A, Scheer A M, Denifl S, Ptasińska S, Märk T D and Scheier P 2006 *J. Chem. Phys.* **124** 124310
Caminati W 2009 *Angew. Chem. Int. Ed. Engl.* **48** 9030
Carr J M, Galiatsatos P G, Gorfinkiel J D, Harvey A G, Lysaght M A, Madden D, Masin Z, Plummer M and Tennyson J 2012 *Euro. J. Phys.* D **66** 58
Chu S I and Dalgarno A 1974 *Phys. Rev.* A **10** 788
Denifl S, Ptasińska S, Hanel G, Stir B, Probst M, Scheier P and Märk T D 2003 *J. Chem. Phys.* **120** 6557
Denifl S, Ptasińska S, Probst M, Hrusák J, Scheier P and Märk T D 2004 *J. Phys. Chem.* A **108** 6562–9
Dora A, Bryjko L, van Mourik T and Tennyson J 2012 *J. Chem. Phys.* **136** 024324
Dora A, Tennyson J, Bryjko L and van Mourik T 2009 *J. Chem. Phys.* **130** 164307
Faure A, Gorfinkiel J D, Morgan L A and Tennyson J 2002 *Comput. Phys. Commun.* **144** 224–41
Frisch M J *et al* 2004 *Gaussian 03, Revision C.02* (Wallingford, CT: Gaussian Inc.)
Fülscher M P and Roos B O 1995 *J. Am. Chem. Soc.* **117** 2089–95
García Gómez-Tejedor G and Fuss M C (ed) 2012 *Radiation Damage in Biomolecular Systems Biological and Medical Physics Biomedical Engineering* (Dordrecht: Springer)
Gianturco F A, Sebastianelli F, Lucchese R R, Baccareli I and Sanna N 2008 *J. Chem. Phys.* **128** 174302
Gorfinkiel J D and Tennyson J 2004 *J. Phys. B: At. Mol. Opt. Phys.* **37** L343–50
Gorfinkiel J D and Tennyson J 2005 *J. Phys. B: At. Mol. Opt. Phys.* **38** 1607–22
Hanel G, Stir B, Denifl S, Scheier P, Probst M, Farizon B, Farizon M, Illenberger E and Märk T D 2003 *Phys. Rev. Lett.* **90** 188104
Levesque P L, Michaud M, Cho W and Sanche L 2005 *J. Chem. Phys.* **122** 224704
Lorentzon J, Fülscher M P and Roos B O 1995 *J. Am. Chem. Soc.* **117** 9265–73
Mašín Z and Gorfinkiel J D 2011 *J. Chem. Phys.* **135** 144308
Morgan L A, Tennyson J and Gillan C J 1998 *Comput. Phys. Commun.* **114** 120
Ptasińska S, Denifl S, Mróz B, Probst M, Grill V, Illenberger E, Scheier P and Märk T D 2005 *J. Chem. Phys.* **123** 124302
Renjith B, Bhowmick S, Mishra M K and Sarma M 2011 *J. Phys. Chem.* A **115** 13753
Scheer A M, Aflatooni K, Gallup G A and Burrow P D 2004 *Phys. Rev. Lett.* **92** 068102
Scheer A M, Silvernail C, Belot J A, Aflatooni K, Gallup G A and Burrow P D 2005 *Chem. Phys. Lett.* **411** 46
Stibbe D T and Tennyson J 1996 *J. Phys. B: At. Mol. Opt. Phys.* **29** 4267
Stibbe D T and Tennyson J 1997 *J. Phys. B: At. Mol. Opt. Phys.* **30** L301–7
Tarana M and Tennyson J 2008 *J. Phys. B: At. Mol. Opt. Phys.* **41** 205204
Tennyson J 1996 *J. Phys. B: At. Mol. Opt. Phys.* **29** 6185–201
Tennyson J 2004 *J. Phys. B: At. Mol. Opt. Phys.* **37** 1061–71
Tennyson J 2010 *Phys. Rep.* **491** 29–76
Tennyson J and Noble C J 1984 *Comput. Phys. Commun.* **33** 421–4
Tonzani S and Greene C H 2006a *J. Chem. Phys.* **124** 054312
Tonzani S and Greene C H 2006b *J. Chem. Phys.* **125** 094504
Trevisan C S, Orel A E and Rescigno T N 2006 *J. Phys. B: At. Mol. Opt. Phys.* **39** L255–60
Varsano D, Felice R D, Marques M A L and Rubio A 2006 *J. Phys. Chem.* B **110** 7129–38

Wang Y F and Tian S X 2011 *Phys. Chem. Chem. Phys.* **13** 6169–75
Werner H J *et al* 2006 Molpro, version 2006.1 (a package of *ab initio* programs) http://www.molpro.net
Winstead C and McKoy V 2006a *J. Chem. Phys.* **125** 244302
Winstead C and McKoy V 2006b *J. Chem. Phys.* **125** 174304
Winstead C and McKoy V 2007a *J. Chem. Phys.* **127** 085105
Winstead C and McKoy V 2007b *Phys. Rev.* A **76** 012712
Winstead C and McKoy V 2007c *Phys. Rev. Lett.* **98** 113201
Winstead C and McKoy V 2008a *Int. J. Mass Spectrom.* **277** 279
Winstead C and McKoy V 2008b *Rad. Phys. Chem.* **77** 1258
Zhang R, Galiatsatos P and Tennyson J 2011 *J. Phys. B: At. Mol. Opt. Phys.* **44** 195203